The gas-phase structure of octaphenyloctasilsesquioxane Si8O12Ph8 and the crystal structures of Si8O12(p-tolyl)8 and Si8O12(p-ClCH2C6H4)8

Dalton Transactions

An international journal of inorganic chemistry

www.rsc.org/dalton

Volume 39 | Number 30 | 14 August 2010 | Pages 6893–7168

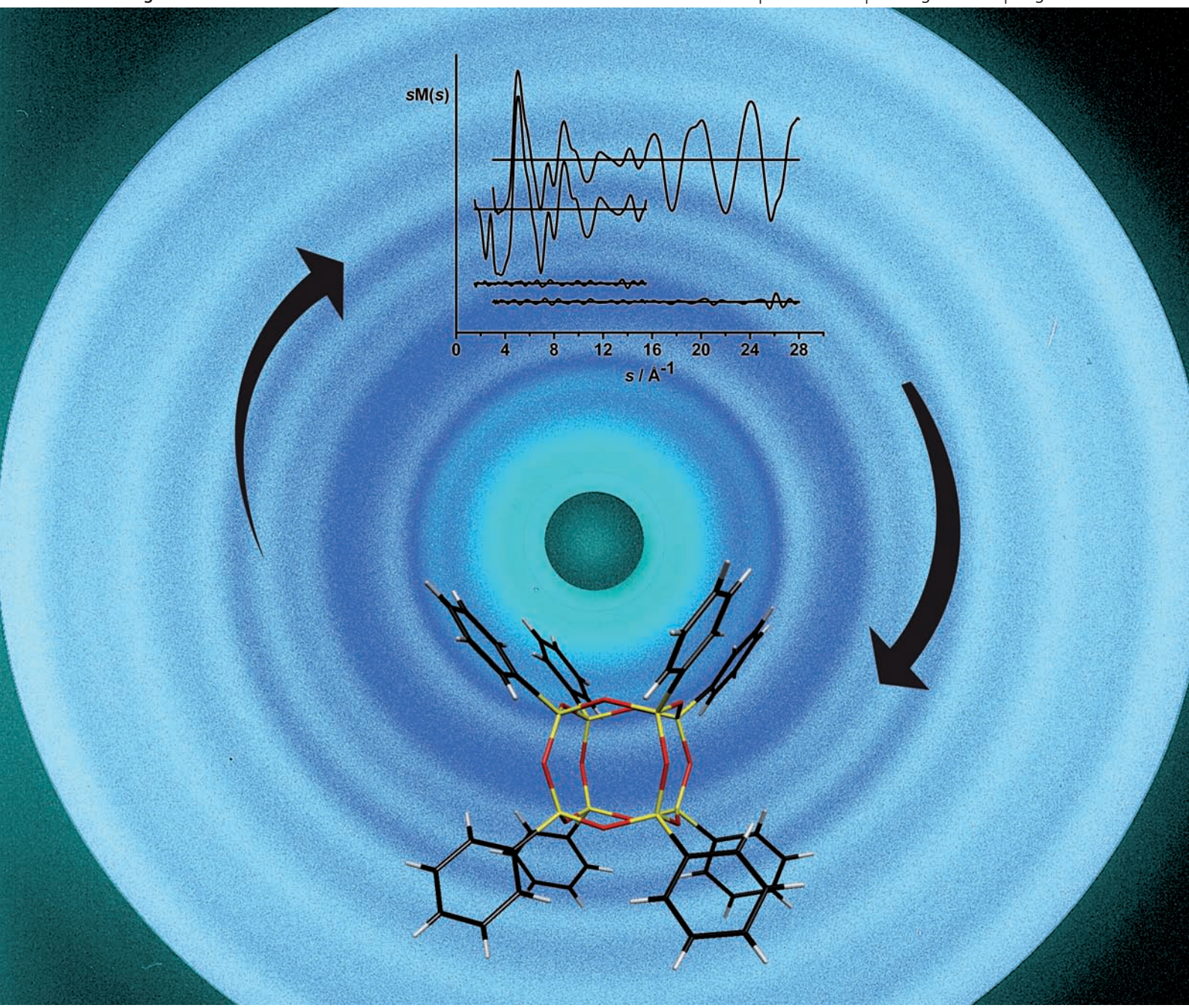

ISSN 1477-9226

RSC Publishing

PAPER

Zakharov, Masters, Lickiss *et al.*
The gas-phase structure of octaphenyloctasilsesquioxane $Si_8O_{12}Ph_8$ and the crystal structures of Si_8O_{12} (*p*-tolyl)$_8$ and Si_8O_{12}(*p*-$ClCH_2C_6H_4$)$_8$

PERSPECTIVE

Schulz *et al.*
Recoverable chiral salen complexes for asymmetric catalysis: recent progress

1477-9226(2010)39:30;1-6

The gas-phase structure of octaphenyloctasilsesquioxane $Si_8O_{12}Ph_8$ and the crystal structures of Si_8O_{12}(*p*-tolyl)$_8$ and Si_8O_{12}(*p*-$ClCH_2C_6H_4$)$_8$†‡

Alexander V. Zakharov,*[a,b] Sarah L. Masters,*[b] Derek A. Wann,[b] Sergei A. Shlykov,[a] Georgiy V. Girichev,[a] Sophie Arrowsmith,[c] David B. Cordes,[c] Paul D. Lickiss*[c] and Andrew J. P. White[c]

Received 15th January 2010, Accepted 9th April 2010
First published as an Advance Article on the web 4th May 2010
DOI: 10.1039/c000664e

The equilibrium molecular structure of octaphenyloctasilsesquioxane $Si_8O_{12}Ph_8$ in the gas phase has been determined by electron diffraction. It was found to have D_4 point-group symmetry, with Si–O bond lengths of 1.634(15)–1.645(19) Å, and a narrow range [147.5(45)–149.8(24)°] of Si–O–Si angles. The structures of Si_8O_{12}(*p*-tolyl)$_8$ and Si_8O_{12}(*p*-$ClCH_2C_6H_4$)$_8$ have been determined by X-ray diffraction and are found to have Si_8O_{12} cages significantly distorted from the symmetry found for $Si_8O_{12}Ph_8$ in the gas phase. Thus, Si–O–Si angles range between 144.2(2)–151.64(16)° for Si_8O_{12}(*p*-tolyl)$_8$, and between 138.8(2)–164.2(2)° for Si_8O_{12}(*p*-$ClCH_2C_6H_4$)$_8$. These three structures show how much a Si_8O_{12} cage may be distorted away from an ideal structure, free from intermolecular forces, by packing forces in a crystalline lattice.

Introduction

Octaphenyloctasilsesquioxane, $Si_8O_{12}Ph_8$ (**1**), is a member of an increasingly widely used group of compounds known as polyhedral oligomeric silsesquioxanes (POSS). The most common members of the POSS family have the general formula $Si_8O_{12}R_8$, where R can be a wide range of alkyl, alkenyl, aryl and siloxy groups. These compounds have found many applications in polymer science and in composite materials, where they have been used to modify mechanical, thermal, optical, dielectric, surface and other properties (for reviews see refs. 1–4).

The phenyl derivative, $Si_8O_{12}Ph_8$, can be readily prepared *via* hydrolysis of either $PhSiCl_3$ or $PhSi(OEt)_3$ (see ref.1 for a comparison of synthetic methods) and can be nitrated[5–8] to give a mixture of isomers. The nitro-derivatives can then be reduced to give a mixture of–NH_2 substituted isomers, which have been used as precursors to a range of novel materials.[1,4] Bromination[9,10] and iodination[11] of $Si_8O_{12}Ph_8$ gives aryl-halide products that can also be used as nano-scale building blocks for new materials.

Several structural studies of $Si_8O_{12}Ph_8$ and related species are detailed in the literature. Although no solvent-free X-ray crystal structure for $Si_8O_{12}Ph_8$ has previously been reported, there are X-ray studies of this molecule in solvates with $C_5H_5N/C_6H_4Cl_2$[12] and $Me_2C{=}O$,[13] and for $[Si_8O_{12}Ph_8F]^-$ in a salt, $[NBu_4][Si_8O_{12}Ph_8F]$.[14] To the best of our knowledge, no previous isolated-molecule studies have been performed, but calculations have been done on the solid-state structure using plane-wave DFT by Lin *et al.*[15] They carried out a computational study of the unsubstituted octahydridosilsesquioxane, $Si_8O_{12}H_8$, several phenyl-substituted silsesquioxanes $Si_8O_{12}H_{8-n}Ph_n$ (n = 1 or 2), and the octaphenyl derivative, $Si_8O_{12}Ph_8$ (**1**). The authors report that the optimised structure of **1** has low symmetry because of the various orientations of the eight phenyl rings. However, they mention that the cell size used is not big enough for such a system and it has reached their current hardware capacity limit. They performed a geometry optimisation for $Si_8O_{12}H_8$ to test the reliability of their methodology and found that the bigger the cell is, the closer to O_h symmetry the optimised structure of $Si_8O_{12}H_8$ will be. As was later determined experimentally, the equilibrium geometry of gas-phase $Si_8O_{12}H_8$ does indeed have O_h symmetry.[16] The lack of symmetry of the $Si_8O_{12}Ph_8$ structure in the study by Lin *et al.*[15] may also have been caused by intermolecular interactions due to the small box size used in the periodic-code calculations.

In order to understand better the nature of an aryl-substituted POSS cage in the absence of packing forces and solvent, and also to make comparison with the gas-phase structures of $Si_8O_{12}H_8$ and $Si_8O_{12}Me_8$,[16] a gas-phase electron-diffraction study was undertaken of $Si_8O_{12}Ph_8$ (**1**). X-ray diffraction structures of Si_8O_{12}(*p*-tolyl)$_8$ (**2**) and Si_8O_{12}(*p*-$ClCH_2C_6H_4$)$_8$ (**3**) have also been determined in order to make comparisons between simple arylsilsesquioxane structures.

Experimental section

Preparation of $Si_8O_{12}Ph_8$ (1)

Although the synthesis of $Si_8O_{12}Ph_8$ is straightforward, the sample used for the electron-diffraction study was purchased from Hybrid Plastics Inc. and was used without further purification.

[a]*Department of Physics, Ivanovo State University of Chemistry and Technology, Engelsa 7, Ivanovo, 153000, Russian Federation. E-mail: a_zakharov@isuct.ru*
[b]*School of Chemistry, University of Edinburgh, West Mains Road, Edinburgh, UK EH9 3JJ. E-mail: s.masters@ed.ac.uk*
[c]*Department of Chemistry, Imperial College London, South Kensington, London, UK SW7 2AZ. E-mail: p.lickiss@imperial.ac.uk*

† Dedicated to Professor David W. H. Rankin on the occasion of his retirement.

‡ Electronic supplementary information (ESI) available: Additional tables and figures. CCDC reference numbers 746535 and 746536. For ESI and crystallographic data in CIF or other electronic format see DOI: 10.1039/c000664e

Preparation of Si_8O_{12}(*p*-tolyl)$_8$ (2)

2 was prepared using the same method as reported for the Si_8O_{12}(*m*-tolyl)$_8$ isomer,[17] giving 0.99 g (0.9% yield) of white microcrystals from the hydrolysis of 23.00 g of (*p*-tolyl)$SiCl_3$. The melting point of the crystals was >360 °C (from Me_2CO/CH_2Cl_2), with literature values for the melting point given as 400 °C (decomp.)[5] and 407–413 °C (decomp.).[18] NMR characterisation of **2** was as follows: ^{1}H NMR (400 MHz, $CDCl_3$) δ 7.65 (2H, d, J = 7.8 Hz, aryl-H), 7.18 (2H, d, J = 7.8 Hz, aryl-H), 2.35 (3H, s, Me). ^{13}C NMR (100 MHz, $CDCl_3$) δ 140.72 (*C*-Me), 134.39, 128.70, 127.16 (aryl C), 21.74 (Me). ^{29}Si NMR (79.5 MHz, $CDCl_3$) δ –77.62 ppm. Crystals suitable for single-crystal X-ray diffraction studies were obtained by slowly adding acetone to a saturated CH_2Cl_2 solution until a 3 : 1 v/v acetone/CH_2Cl_2 solution was formed.

Crystal data for 2. $C_{56}H_{56}O_{12}Si_8 \cdot 6Me_2CO$, M = 1494.20, tetragonal, $I4/m$ (no. 87), $a = b$ = 19.4815(3), c = 20.9445(4) Å, V = 7949.0(2) Å^3, Z = 4 [C_{2h} symmetry], D_c = 1.249 g cm^{-3}, μ(Cu-Kα) = 1.809 mm^{-1}, T = 173 K, colourless needles, Oxford Diffraction Xcalibur PX Ultra diffractometer; 3830 independent measured reflections (R_{int} = 0.0449), F^2 refinement, R_1(obs) = 0.0626, wR_2(all) = 0.1813, 2579 independent observed absorption-corrected reflections [$|F_o| > 4\sigma(|F_o|)$, $2\theta_{max}$ = 142°], 195 parameters. CCDC 746535.

Preparation of Si_8O_{12}(*p*-$ClCH_2C_6H_4$)$_8$ (3)

3 was prepared according to a literature method,[19] which gave a white crystalline product with spectroscopic data in agreement with those published. Material suitable for study by single-crystal X-ray diffraction was obtained by slowly adding acetone to a saturated CH_2Cl_2 solution until a 3 : 1 v/v acetone/CH_2Cl_2 solution was formed.

Crystal data for 3. $C_{56}H_{48}Cl_8O_{12}Si_8$, M = 1421.26, triclinic, $P\bar{1}$ (no. 2), a = 12.8106(6), b = 13.2923(6), c = 22.1442(10) Å, α = 76.315(4), β = 75.028(4), γ = 61.699(5)°, V = 3178.4(3) Å^3, Z = 2, D_c = 1.485 g cm^{-3}, μ(Mo-Kα) = 0.564 mm^{-1}, T = 173 K, colourless blocks, Oxford Diffraction Xcalibur 3 diffractometer; 10107 independent measured reflections (R_{int} = 0.0521), F^2 refinement, R_1(obs) = 0.0547, wR_2(all) = 0.1349, 4702 independent observed absorption-corrected reflections [$|F_o| > 4\sigma(|F_o|)$, $2\theta_{max}$ = 52°], 777 parameters. CCDC 746536.

Computational studies

Computational studies of $Si_8O_{12}Ph_8$ (**1**) were carried out using density functional theory (DFT) calculations utilising the B3LYP hybrid functional (Becke + Slater + HF exchange and LYP + VWN5 correlation).[20] Preliminary calculations, intended for obtaining starting geometries and Hessian matrices for higher-level computations, as well as for evaluation of vibrational correlation, were carried out using the 6-31G basis sets.[21] In the final calculations, all atoms were described by the triple-ζ valence correlation-consistent cc-pVTZ basis sets.[22] The basis sets in the GAMESS format were obtained using basis set exchange (BSE) software and the EMSL basis set library.[23] All calculations were performed using PC GAMESS Version 7.0[24] of the GAMESS software package.[25]

Preliminary calculations showed that there are two conformers of $Si_8O_{12}Ph_8$ (with D_4 and D_{2d} symmetries) having almost the same energy, with a few vibrational frequencies with values close to zero. All other structures with higher symmetries have significantly higher energies and are saddle points with multiple imaginary frequencies corresponding to rotations of the phenyl rings. In our experience, DFT calculations have been found to be prone to producing spurious imaginary frequencies with magnitudes of less than 10 cm^{-1}. Therefore we used HF analytic force field calculations (which do not produce spurious imaginary frequencies) in addition to the DFT calculations with different basis sets to determine whether the structures with D_4 and D_{2d} symmetries are minima or saddle points.

Gas electron diffraction

The diffraction patterns for $Si_8O_{12}Ph_8$ were obtained in a synchronous gas electron diffraction (GED) and mass spectrometric (MS) experiment carried out using the EMR-100/APDM-1 unit[26] at the Ivanovo State University of Chemistry and Technology. A sample of **1** was evaporated at temperature T = 615(10) K from a stainless-steel cell with a cylindrical effusion nozzle of 0.6 × 1.2 mm size (diameter × length). The ratio of the evaporation area to the effusion orifice area was above 500. The mass spectrum of the saturated vapour over the sample showed a molecular ion of stable intensity, indicating the presence of the molecular species in the vapour at the temperature of the experiment. The vapour composition was monitored by mass spectrometry throughout the experiment.

Electron-diffraction patterns were obtained for both short (L_1 = 338 mm) and long (L_2 = 598 mm) nozzle-to-camera distances at accelerating voltages of 73 and 74 kV, respectively. Accurate wavelengths of electrons have been calibrated using polycrystalline ZnO. The diffraction patterns were recorded using Kodak SO-163 electron image films, which were scanned using a calibrated Epson Expression 1680 Pro flatbed scanner in a procedure documented elsewhere.[27] A data-reduction procedure described in detail in ref.28 was employed. The least-squares structure refinement was performed using a modified version of the KCED 35 program.[29] Scattering functions were calculated from tabulated atomic scattering factors.[30]

Nozzle-to-plate distances (mm), temperatures (K), accelerating voltages (kV), individual R-factors, scale factors and electron wavelengths (Å^{-1}) for each camera distance are given in the Supplementary Information (Table S1).‡

Results and discussion

Computational studies of $Si_8O_{12}Ph_8$ (1)

It was found that the structure of **1** with D_4 symmetry is a minimum, apparently a global one since no structure with a lower energy was found. The D_{2d}-symmetric configuration is a saddle point with four imaginary frequencies (values of i6 to i8 cm^{-1}), corresponding to rotations of the phenyl rings. The structure with D_{2d} symmetry is only marginally higher in energy (ΔE = 0.03 kJ mol^{-1}) than the D_4 structure at the highest level of theory. The latter is the only minimum on the potential-energy

surface (PES) of $Si_8O_{12}Ph_8$, so the GED analysis of $Si_8O_{12}Ph_8$ was performed assuming that only one conformer exists in the vapour.

Despite the presence of such a tiny barrier, there is no free rotation of phenyl rings in $Si_8O_{12}Ph_8$, although the rings do exhibit almost uninhibited large-amplitude twists. The complete rotation of a phenyl ring requires much higher energy due to steric hindrance, as evidenced by our calculations of higher-symmetry structures, where the phenyl rings are unfavourably oriented with respect to each other. The coordinates of **1** from the B3LYP/cc-pVTZ calculation are given in the Supplementary Information (Table S2).‡

GED refinement of $Si_8O_{12}Ph_8$ (1)

Based on the D_4-symmetric structure identified by quantum chemical calculations, a *Z*-matrix model was written to describe the geometry of **1**. The parameters used are shown in Table 1. Silicon and oxygen atom numbering is shown in Fig. 1; all coordinates are listed in Supplementary Information (Table S3).‡

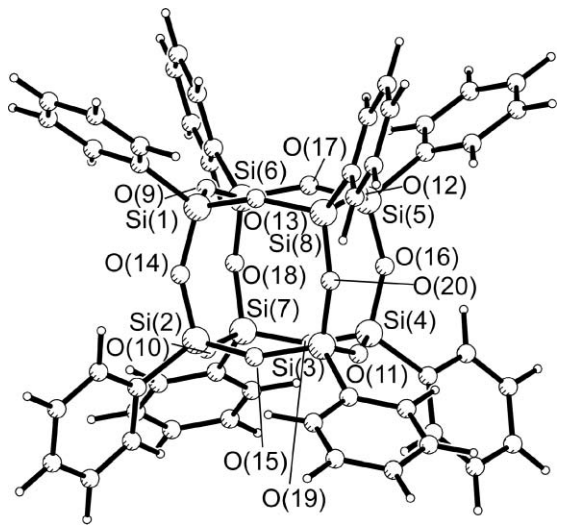

Fig. 1 Molecular structure, including atom numbering, of $Si_8O_{12}Ph_8$ (**1**). Hydrogen and carbon atom numbers have been omitted for clarity.

In order to write the model, seven dummy atoms were defined, one in the origin of coordinates (0_C), and six located on the coordinate axes (which point to the centres of the cube faces), in both positive and negative directions from the coordinate origin. This was done to make it possible to use the same parameters to describe symmetrically equivalent atoms.

The Si(1)–0_C–X angle (p_2) and the Si(1)–0_C–X–Z dihedral angle (p_3) are both fixed to their computed values to match the initial atomic coordinates of the ED model to the result of the B3LYP/cc-pVTZ calculation. They are fixed in order to define the orientation of the molecule and this does not prevent the refinement of other parameters. As O(9) and the symmetry equivalent oxygen atoms have $z = 0$ and $x = 0$ or $y = 0$, there are no refined angles and dihedrals (they are equal to 90°). The C–C distances (p_{11}), except for *r*C(53)–C(61), are refined as a group (since they are close to each other and cannot be determined independently) and the differences between them are fixed to computed (B3LYP/cc-pVTZ) values. *r*C(53)–C(61) is a ring closing parameter determined *via* other C–C distances and C–C–C angles, not differences between C–C distances. The dihedral angles within the phenyl rings are very close to 0 or 180° (*i.e.* the rings are almost planar) and therefore are fixed to computed values. As with the C–C distances, the C–H distances are refined as a group and the small differences between them are fixed to computed values. As it is unlikely that they could be reliably refined, the H–C–C angles and H–C–C–C dihedral angles are fixed to computed values.

The final *R* factor for the refinement is 5.3%. The quality of the refinement can be seen by looking at the radial-distribution curve shown in Fig. 2. The molecular-scattering intensity curves are shown in Figure S1. The correlation matrices are given in Tables S4 and S5, and a full list of distances with amplitudes of vibration and

Table 1 Geometric parameters from the GED refinement (r_{h1}) of $Si_8O_{12}Ph_8$ (**1**) and their calculated equivalents (r_e; B3LYP/cc-pVTZ)[a]

	Parameter	r_{h1}	r_e
Independent			
p_1	*r*Si(1)–0_C[b]	2.737(1)	2.737
p_2	∠Si(1)–0_C–X[c]	124.8(fixed)	124.8
p_3	*ϕ*Si(1)–0_C–X–Z[d]	45.4(fixed)	45.4
p_4	*r*O(9)–0_C	2.695(20)	2.676
p_5	*r*O(13)–Si(1)	1.634(8)	1.637
p_6	∠O(13)–Si(8)–O(12)	108.3(2)	108.3
p_7	*ϕ*O(13)–Si(8)–O(12)–0_C	−60.1(fixed)	−60.1
p_8	*r*Si(1)–C(21)	1.859(1)	1.857
p_9	∠C(21)–Si(1)–O(13)	110.2(16)	109.4
p_{10}	*ϕ*C(21)–Si(1)–O(13)–0_C	−179.7(fixed)	−179.7
p_{11}	*r*C–C mean	1.395(2)	1.401
p_{12}	∠C(29)–C(21)–Si(1)	119.8(8)	120.8
p_{13}	*ϕ*C(29)–C(21)–Si(1)–O(9)	37.0(48)	37.0
p_{14}	∠C(37)–C(21)–Si(1)	122.2(9)	121.0
p_{15}	*ϕ*C(37)–C(21)–Si(1)–O(9)	−145.5(31)	−142.7
p_{16}	∠C(45)–C(29)–C(21)	121.9(12)	121.0
p_{17}	*ϕ*C(45)–C(29)–C(21)–C(37)	−0.21(fixed)	−0.21
p_{18}	∠C(53)–C(37)–C(21)	120.8(13)	120.9
p_{19}	*ϕ*C(53)–C(37)–C(21)–C(29)	0.23(fixed)	0.23
p_{20}	∠C(61)–C(45)–C(29)	119.7(14)	120.0
p_{21}	*r*C–H mean	1.073(2)	1.082
Dependent			
p_{22}	*r*C(29)–C(45)	1.384(5)	1.390
p_{23}	*r*C(53)–C(61)	1.402(27)	1.390
p_{24}	*r*C(37)–C(53)	1.385(5)	1.390
p_{25}	*r*C(45)–C(61)	1.385(5)	1.391
p_{26}	*r*C(21)–C(37)	1.395(5)	1.400
p_{27}	*r*C(21)–C(29)	1.395(5)	1.401
p_{28}	*r*Si(1)–O(13)	1.634(15)	1.637
p_{29}	*r*Si(1)–O(9)	1.645(19)	1.639
p_{30}	*r*Si(1)–O(14)	1.641(24)	1.642
p_{31}	*r*Si(1)–C(21)	1.859(3)	1.857
p_{32}	∠Si(1)–O(13)–Si(8)	149.8(24)	149.2
p_{33}	∠O(13)–Si(1)–O(14)	108.9(7)	108.9
p_{34}	∠O(13)–Si(1)–O(9)	110.3(5)	110.2
p_{35}	∠O(14)–Si(1)–O(9)	108.3(6)	108.3
p_{36}	∠Si(1)–O(9)–Si(6)	147.5(45)	148.8
p_{37}	∠O(13)–Si(1)–C(21)	110.2(49)	109.4
p_{38}	∠Si(1)–C(21)–C(37)	122.2(26)	121.0
p_{39}	∠Si(1)–C(21)–C(29)	119.8(24)	120.8
p_{40}	∠C(21)–C(37)–C(53)	120.8(38)	120.9
p_{41}	∠C(21)–C(29)–C(45)	121.9(38)	121.0
p_{42}	∠C(29)–C(45)–C(61)	119.7(50)	120.0
p_{43}	∠C(37)–C(53)–C(61)	120.4(33)	120.0
p_{44}	∠C(45)–C(61)–C(53)	119.3(14)	119.8
p_{45}	∠C(29)–C(21)–C(37)	118.0(10)	118.2

[a] Distances (*r*) are in Å, angles (∠) and dihedral angles (*ϕ*) are in degrees. [b] 0_C is the centre of the coordinate system. [c] X is a dummy atom on the positive *x* axis. [d] Z is a dummy atom on the positive *z* axis.

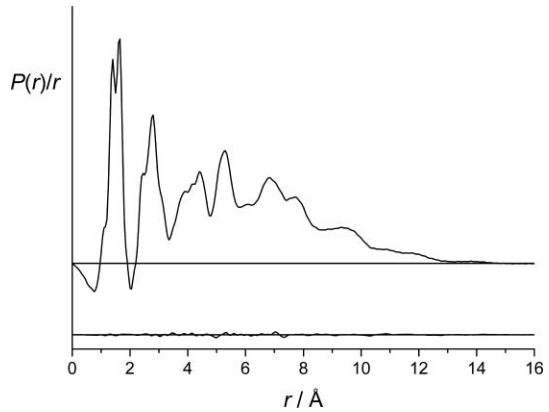

Fig. 2 The radial distribution curve for the GED refinement of $Si_8O_{12}Ph_8$ (**1**).

distance corrections is shown in Table S6. The final coordinates for the GED-refined structure of **1** are given in Table S3, with those calculated at the B3LYP/cc-pVTZ level given in Table S2.‡

Despite efforts to improve the agreement between the theoretical and experimental intensities, the *R* factor remained relatively high. The main reason for this discrepancy is the very large and highly anharmonic rotations of the phenyl rings, which produce probability distribution functions for corresponding internuclear distances that are quite unusual.

The average probability distribution function used in the calculation of the molecular-scattering intensity is a Gaussian function with the root-mean-square vibrational amplitude as its variance parameter.[31] In the general case of anharmonic vibrations it is possible to represent the probability distribution function as a somewhat distorted Gaussian function,[31,32] but in all presently used least-squares codes for the analysis of ED data only the asymmetry constant, related to Morse constant of the anharmonic potential,[31] is implemented.

In previous studies of related silsesquioxanes in the gas phase we have performed molecular-dynamics (MD) simulations to study the probability distribution functions of pairs of atoms.[16,33-35] Here again we have used MD to observe the shapes of the probability distribution functions. Semi-empirical molecular-dynamics (SE-MD) calculations for **1** were performed using the resources of the EaStCHEM research computing facility[36] running the CP2K code.[37] A geometry optimisation was initially carried out using the PM6 method,[38] before the optimised geometry was used as the starting geometry for an SE-MD simulation in the NVT ensemble. The canonical sampling *via* velocity rescaling (CSVR) thermostat was used to control the temperature.[39] A time step of 0.5 fs was used and the simulation was run for 30 ps. This methodology has already been shown to give accurate results for other substituted silsesquioxanes.[35] Fig. 3(a) shows the probability distribution function for *r*Si(1)–C(68), extracted from the molecular-dynamics simulation. [C(68) is the carbon atom in the *para* position on a phenyl ring attached to a silicon atom that is two bonds away from Si(1).] Despite the expected large-amplitude wagging of the phenyl rings, the distribution can be described sufficiently well by a Gaussian function. The probability distribution function for *r*Si(1)–C(52) is presented in Fig. 3(b). [C(52) is a carbon atom in the *meta* position in the same phenyl ring as C(68).] It can be seen that the distribution is very unusual and it follows that the corresponding molecular-scattering intensity term cannot be properly described by the Gaussian approximation used in existing refinement programs. As the corresponding potential is also not a Morse potential, the inclusion of the asymmetry constant is not enough to correct this problem and higher-order corrections are necessary. The data required to perform the higher-order corrections are available from the MD simulations, but no least-squares software exists that can use it.

Although the distances between silicon or oxygen atoms and carbon atoms in the rotating parts of the phenyl rings are mostly larger than 4 Å [the exceptions are Si(1)–C(29) and Si(1)–C(37)], their contributions to the molecular-scattering function are not negligible. It is this insufficiently accurate calculation of the theoretical intensity functions that has led to a larger-than-normal disagreement with the experimental data.

Solid-state structures of Si_8O_{12}(*p*-tolyl)$_8$ (2) and Si_8O_{12}(*p*-$ClCH_2C_6H_4$)$_8$ (3)

Several solid-state structural studies have previously been performed for $Si_8O_{12}Ph_8$ (**1**) and the related endohedral anion

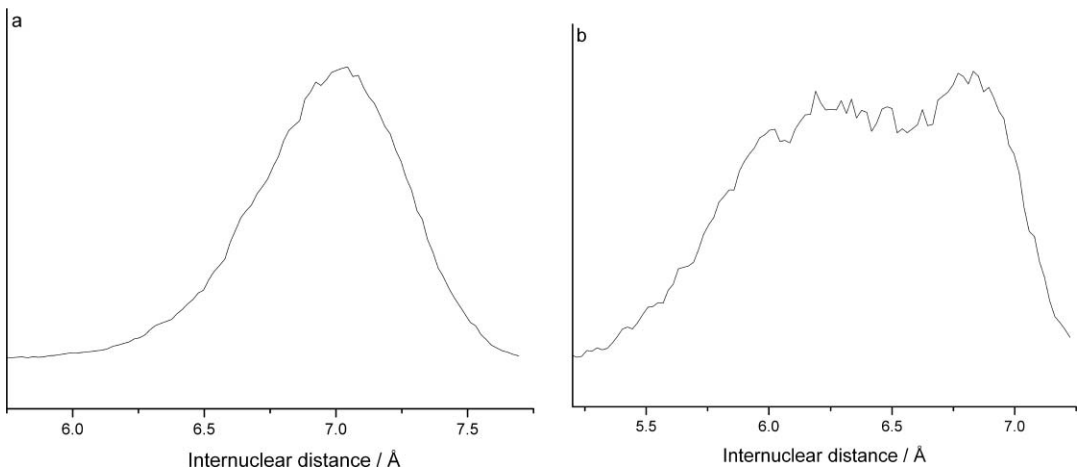

Fig. 3 Probability distribution functions for (a) *r*Si(1)–C(68) and (b) *r*Si(1)–C(52), extracted from the molecular-dynamics simulation. The *y* axis is the probability (normalised so the sum of all probabilities is equal to unity).

Table 2 Selected calculated and experimental solid-state structural data for $Si_8O_{12}Ar_8$ and $[Si_8O_{12}Ar_8F]^-$ compounds[a]

Compound	Method	*r*Si–O/Å		∠Si–O–Si (°)		Ref.
		Range	mean	Range	mean	
$Si_8O_{12}Ph_8$[b]	Calc.	1.603–1.614	1.609	145.4–152.8	149.5	15
$Si_8O_{12}Ph_8$	GED	1.634(15)–1.645(19)	1.640	147.5(45)–149.8(24)	149.0	This work
$Si_8O_{12}Ph_8$ ($C_5H_5N/C_6H_4Cl_2$ solvate)	X-ray	1.606(5)–1.621(5)	1.614	143.9(3)–156.6(4)	149.2	12
$Si_8O_{12}Ph_8$ ($Me_2C{=}O$ solvate)	X-ray	1.606(3)–1.618(3)	1.612	144.7(2)–151.6(2)	149.2	13
$[NBu_4][Si_8O_{12}Ph_8F]$	X-ray	1.6198(15)–1.6295(15)	1.6248	138.56(10)–143.88(10)	141.18	14
$Si_8O_{12}(p\text{-tolyl})_8$ ($Me_2C{=}O$ solvate)	X-ray	1.611(2)–1.623(3)	1.616	144.2(2)–151.64(16)	148.1	This work
$[NBu_4][Si_8O_{12}(p\text{-tolyl})_8F]$	X-ray	1.6234(19)–1.628(2)	1.625	140.50(13)–142.47(13)	141.17	42
$Si_8O_{12}(o\text{-tolyl})_8$	X-ray	1.6119(15)–1.6257(15)	1.6188	139.01(11)–163.34(11)	149.22	43
$Si_8O_{12}(o\text{-}Me_2NC_6H_4)_8$	X-ray	1.611(1)–1.626(2)	1.617	143.5(1)–155.2(1)	148.42	44
$Si_8O_{12}(p\text{-}ClCH_2C_6H_4)_8$	X-ray	1.602(3)–1.627(4)	1.617	138.8(2)–164.2(2)	148.7	This work
$Si_8O_{12}(p\text{-}IC_6H_4)_8$ (EtOAc solvate)	X-ray	1.603(4)–1.616(4)	1.610	144.7(4)–152.0(3)	148.0	11

[a] Table adapted from ref.1. [b] Geometry optimisation using CASTEP GGA-PW91.

$[Si_8O_{12}Ph_8F]^-$, and selected data are given in Table 2. It should be noted that an early X-ray diffraction study found that two forms of $Si_8O_{12}Ph_8$ could be obtained from pyridine, one with a triclinic and one a monoclinic unit cell.[40]

The calculated Si–O bond lengths and Si–O–Si bond angles agree well with experimentally determined values obtained by single-crystal X-ray crystallography and also show the low symmetry caused by the various orientations of the Ph substituents. Although $Si_8O_{12}R_8$ derivatives are, ideally, highly symmetrical, the Si–O–Si angles are found to vary significantly due to packing of the polyhedra so as to reduce voids within the lattice. This phenomenon has been noted for other members of the $Si_8O_{12}R_8$ family and the effect has been described in detail previously.[1,4,41] The rigidity of the Ph substituents in $Si_8O_{12}Ph_8$ seems to allow voids to occur and these are occupied by the solvent as found in all the solid-state structures listed in Table 2. (In the structure of $[NBu_4][Si_8O_{12}Ph_8F]^-$ the $[NBu_4]^+$ cation sits neatly into a cleft formed by the Ph groups.) The inclusion of solvent is also seen in $Si_8O_{12}(p\text{-}IC_6H_4)_8{\cdot}EtOAc$.[11] Two further simple arylsilsesquioxanes, $Si_8O_{12}(p\text{-tolyl})_8$ (**2**) and $Si_8O_{12}(p\text{-}ClCH_2C_6H_4)_8$ (**3**) have now been structurally characterised by single crystal X-ray diffraction in order to make comparisons with $Si_8O_{12}Ph_8$.

The tolyl derivative, **2**, can be prepared in low yield by hydrolysis of *p*-tolylSiCl$_3$ [5,18] and its structure has been the subject of a previous X-ray crystallographic study which found an orthorhombic unit cell for a crystal obtained from EtOAc.[40] In our hands, **2** crystallised from $Me_2C{=}O/CH_2Cl_2$ solution to give a tetragonal unit cell and the structure is shown in Fig. 4 together with an atom numbering scheme for the Si_8O_{12} cage (which has C_{2h} symmetry), and selected bond lengths and angles are given in Table 3. (Full details of the crystallographic studies can be found in the Electronic Supplementary Information.) The bond lengths within the Si_8O_{12} cage given in Table 3 cover a narrow range and are similar to those for other arylsilsesquioxanes as shown in Table 2. The Si–O–Si angles in the Si_8O_{12} cage range from 144.2(3) to 151.64(16)° and again show the cage to be distorted away from the ideal cubic arrangement of Si atoms as seen in other arylsilsesquioxanes (see Table 2) and also similar to the distortions seen in a wide range of other $Si_8O_{12}R_8$ compounds.[1,4] The crystals for the diffraction study of $Si_8O_{12}(p\text{-tolyl})_8$ were found to contain six molecules of highly disordered acetone per silsesquioxane cage which were removed in the refinement using the SQUEEZE routine of PLATON.[45] This is thus another simple $Si_8O_{12}Ar_8$ compound in which voids between the cages are readily filled by solvent.

Table 3 Selected bond lengths (Å) and angles (°) for **2**[a,b]

Distances			
Si(1)–O(1)	1.619(3)	Si(1)–O(2)	1.611(2)
Si(1)–O(2A)	1.611(2)	Si(2)–O(2)	1.614(2)
Si(2)–O(3)	1.6173(11)	Si(2)–O(4)	1.616(2)
Si(3)–O(4)	1.617(2)	Si(3)–O(4A)	1.617(2)
Si(3)–O(1B)	1.623(3)	O(1)–Si(3B)	1.623(3)
O(3)–Si(2C)	1.6173(11)		
Angles			
O(2)–Si(1)–O(2A)	109.89(17)	O(1)–Si(1)–O(2)	108.76(11)
O(1)–Si(1)–O(2A)	108.76(11)	O(2)–Si(2)–O(3)	109.16(10)
O(2)–Si(2)–O(4)	109.18(12)	O(3)–Si(2)–O(4)	108.63(10)
O(4)–Si(3)–O(4A)	108.19(17)	O(4A)–Si(3)–O(1B)	109.60(11)
O(4)–Si(3)–O(1B)	109.60(11)	Si(1)–O(1)–Si(3B)	144.2(2)
Si(1)–O(2)–Si(2)	151.23(15)	Si(2)–O(3)–Si(2C)	145.16(19)
Si(2)–O(4)–Si(3)	151.64(16)		

[a] See Fig. 4 for atom numbering. [b] The atoms with labels ending in "A", "B" and "C" are related to their counterparts without the suffix by the symmetry operators (x, y, 1–z), (1–x, –y, 1–z) and (1–x, –y, z) respectively.

The molecular structure of $Si_8O_{12}(p\text{-}ClCH_2C_6H_4)_8$ (**3**) is shown in Fig. 5 together with an atom numbering scheme for the Si_8O_{12} cage, and selected bond lengths and angles are given in Table 4. (There is some disorder of two of the $C_6H_4CH_2Cl$ groups which is described in detail in the Electronic Supplementary Information.) The structure is triclinic and again, although the Si–O bond distances within the cage fall in the narrow range of 1.602(3) to 1.627(4) Å the Si–O–Si angles vary widely from 138.8(2) to 164.2(2)°. In this case there is no solvent included in the structure. Although the Si–O–Si angles vary significantly, the O–Si–O angles (shown in Table 4) are all close to the ideal tetrahedral value. It should be noted that the structure of $Si_8O_{12}(p\text{-}ClCH_2C_6H_4)_8$ has been the subject of a previous study which found the compound to crystallise from $Me_2C{=}O/CH_2Cl_2$ in the space group $R\bar{3}$ with $a = b = 13.2961(25)$ and $c = 32.9743(97)$ Å, but disorder of the $C_6H_4CH_2Cl$ groups along the three-fold axis prevented a satisfactory structure solution.[19]

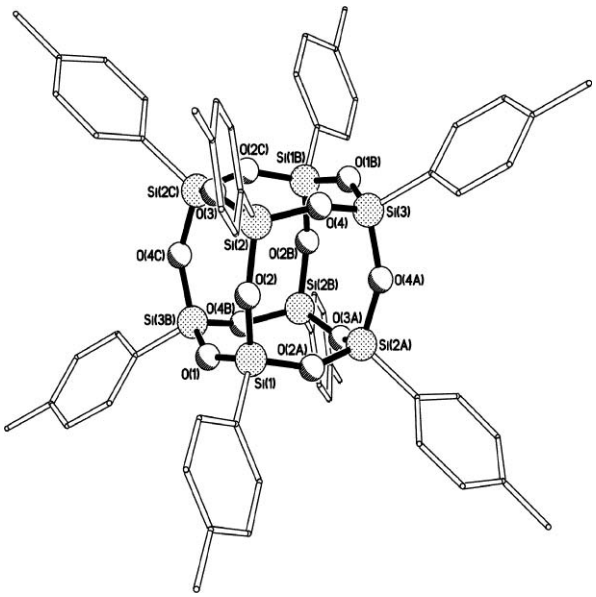

Fig. 4 The molecular structure of the C_{2h} symmetric cage **2**, with atom numbering. The C_2 axis is coincident with the O(3)···O(3A) vector, and Si(1), Si(3), O(1), Si(1A), Si(3A) and O(1A) all lie on the mirror plane. Hydrogen atoms are omitted for clarity.

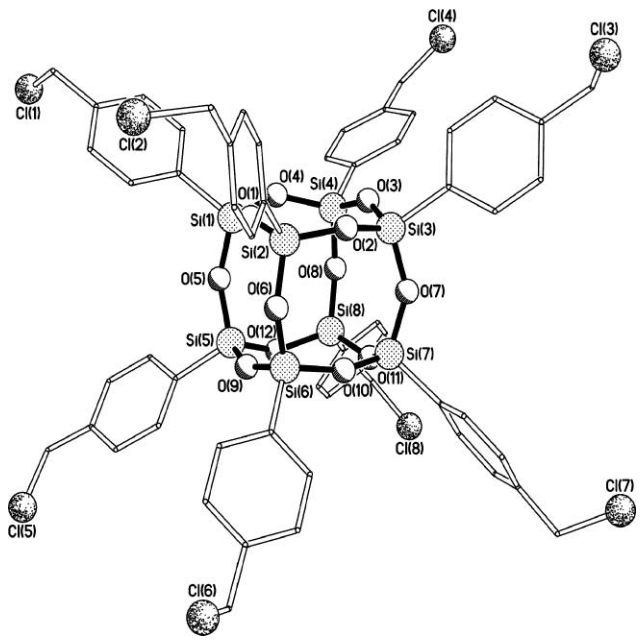

Fig. 5 The molecular structure of **3**, including atom numbering. Hydrogen atoms are omitted for clarity.

These two new X-ray structures are thus both similar to previously reported $Si_8O_{12}R_8$ structures in having cages that are distorted away from the ideal cube, and are in contrast to the structure of $Si_8O_{12}Ph_8$ (**1**) in the gas phase where the lack of crystal packing allows a more symmetrical cage to be favoured. Unlike previous isolated-molecule studies of silsesquioxanes,[16,34] **1** is not found to exist in the highest possible symmetry. It is probably steric effects of the phenyl groups that prevent a conformer with D_{4h} or D_{2d} symmetries from existing as minima on the potential-energy surface. O_h symmetry is not possible for **1**, due to the nature of the substituents.

Table 4 Selected bond lengths (Å) and angles (°) for **3**[a]

Distances			
Si(1)–O(1)	1.618(3)	Si(1)–O(4)	1.617(3)
Si(1)–O(5)	1.610(3)	Si(2)–O(1)	1.612(3)
Si(2)–O(2)	1.627(4)	Si(2)–O(6)	1.619(4)
Si(3)–O(2)	1.619(4)	Si(3)–O(3)	1.615(3)
Si(3)–O(7)	1.620(4)	Si(4)–O(3)	1.619(3)
Si(4)–O(4)	1.626(4)	Si(4)–O(8)	1.602(3)
Si(5)–O(5)	1.618(3)	Si(5)–O(9)	1.611(3)
Si(5)–O(12)	1.622(4)	Si(6)–O(6)	1.618(3)
Si(6)–O(9)	1.616(3)	Si(6)–O(10)	1.618(4)
Si(7)–O(7)	1.624(4)	Si(7)–O(10)	1.607(3)
Si(7)–O(11)	1.625(3)	Si(8)–O(8)	1.612(4)
Si(8)–O(11)	1.626(3)	Si(8)–O(12)	1.613(4)
Angles			
O(1)–Si(1)–O(4)	109.51(18)	O(1)–Si(1)–O(5)	107.93(18)
O(4)–Si(1)–O(5)	109.98(18)	O(1)–Si(2)–O(2)	108.60(18)
O(1)–Si(2)–O(6)	110.68(18)	O(2)–Si(2)–O(6)	108.80(19)
O(2)–Si(3)–O(3)	108.55(18)	O(2)–Si(3)–O(7)	109.42(18)
O(3)–Si(3)–O(7)	109.97(18)	O(3)–Si(4)–O(4)	108.98(18)
O(3)–Si(4)–O(8)	108.29(18)	O(4)–Si(4)–O(8)	107.35(18)
O(5)–Si(5)–O(9)	110.22(18)	O(5)–Si(5)–O(12)	108.56(18)
O(9)–Si(5)–O(12)	108.14(18)	O(6)–Si(6)–O(9)	107.64(19)
O(6)–Si(6)–O(10)	109.01(18)	O(9)–Si(6)–O(10)	109.44(18)
O(7)–Si(7)–O(10)	107.37(18)	O(7)–Si(7)–O(11)	110.73(18)
O(10)–Si(7)–O(11)	109.78(18)	O(8)–Si(8)–O(11)	106.96(18)
O(8)–Si(8)–O(12)	111.40(18)	O(11)–Si(8)–O(12)	108.50(18)
Si(1)–O(1)–Si(2)	155.3(2)	Si(2)–O(2)–Si(3)	147.6(2)
Si(3)–O(3)–Si(4)	146.3(2)	Si(1)–O(4)–Si(4)	138.8(2)
Si(1)–O(5)–Si(5)	152.5(2)	Si(2)–O(6)–Si(6)	142.1(2)
Si(3)–O(7)–Si(7)	147.9(2)	Si(4)–O(8)–Si(8)	164.2(2)
Si(5)–O(9)–Si(6)	150.6(2)	Si(6)–O(10)–Si(7)	154.9(2)
Si(7)–O(11)–Si(8)	141.2(2)	Si(5)–O(12)–Si(8)	142.9(2)

[a] See Fig. 5 for atom numbering.

Conclusion

The equilibrium molecular structure determination of $Si_8O_{12}Ph_8$ in the gas phase by electron diffraction is the first such structure to be determined for a Si_8O_{12} cage with substituents larger than methyl. The narrow range for the Si–O–Si angles [147.5(45)–149.8(24)°], unlike the wide ranges for such angles in most crystalline $Si_8O_{12}R_8$ derivatives, is presumably due to the lack of intermolecular packing forces in the gas phase. The solid-state structures of $Si_8O_{12}(p\text{-tolyl})_8$ and $Si_8O_{12}(p\text{-}ClCH_2C_6H_4)_8$ do show the range of Si–O–Si angles [144.2(2)–151.64(16)° and 138.8(2)–164.2(2)°, respectively] usually found for $Si_8O_{12}R_8$ derivatives and show how much a Si_8O_{12} cage may be distorted away from an ideal structure by packing forces in a crystalline lattice. A flattening in a crystalline lattice of the ideal cubic structure avoids large voids in the lattice and can be accommodated relatively easily due to the flexibility of the Si–O–Si linkage.

Acknowledgements

P. D. L. and D. B. C. thank the UK Energy Research Centre for funding. D. A. W. thanks the EPSRC for funding (EP/F037317); this grant also made it possible for A. V. Z.

to visit Edinburgh for collaborative purposes. We thank Dr Anthony M. Reilly for his assistance with running molecular-dynamics simulations, and the EaStCHEM Research Computing Facility (www.eastchem.ac.uk/rcf), which is partially supported by the eDIKT initiative (http://www.edikt.org), for providing computational resources. S. L. M. thanks the Royal Society of Edinburgh for the award of a personal RSE/BP Fellowship, the EPSRC for funding (EP/D057167/1) and the University of Edinburgh Moray Endowment Fund for sponsoring the visit to Ivanovo to collect electron diffraction data.

References

1 P. D. Lickiss and F. Rataboul, *Adv. Organomet. Chem.*, 2008, **57**, 1.
2 G. Li and C. U. Pittman Jr., in *Macromolecules Containing Metal and Metal-Like Elements*, ed. A. S. Abd-El-Aziz, C. E. Carraher, C. U. Pittman Jr. and M. Zeldin, Wiley, Weinheim, Germany, 2005; vol. 4, Group IVA Polymers, pp. 79-131.
3 R. M. Laine, *J. Mater. Chem.*, 2005, **15**, 3725.
4 D. B. Cordes, P. D. Lickiss and F. Rataboul, *Chem. Rev.*, 2010, **110**, 2081.
5 K. Olsson and C. Grönwall, *Ark. Kemi*, 1961, **17**, 529.
6 S. G. Kim, J. Choi, R. Tamaki and R. M. Laine, *Polymer*, 2005, **46**, 4514.
7 K. Takahashi, S. Sulaiman, J. M. Katzenstein, S. Snoblen and R. M. Laine, *Aust. J. Chem.*, 2006, **59**, 564.
8 H. -J. Chen, *Chem. Res. Chin. Univ.*, 2004, **20**, 42.
9 C. M. Brick, R. Tamaki, S. -G. Kim, M. Z. Asuncion, M. Roll, T. Nemoto, Y. Ouchi, Y. Chujo and R. M. Laine, *Macromolecules*, 2005, **38**, 4655.
10 C. He, Y. Xiao, J. Huang, T. Lin, K. Y. Mya and X. Zhang, *J. Am. Chem. Soc.*, 2004, **126**, 7792.
11 M. F. Roll, M. Z. Asuncion, J. Kampf and R. M. Laine, *ACS Nano*, 2008, **2**, 320.
12 V. E. Shklover, Yu. T. Struchkov, N. N. Makarova and K. A. Andrianov, *J. Struct. Chem.*, 1979, **19**, 944.
13 M. A. Hossain, M. B. Hursthouse and K. M. A. Malik, *Acta Crystallogr., Sect. B: Struct. Crystallogr. Cryst. Chem.*, 1979, **35**, 2258.
14 A. R. Bassindale, M. Pourny, P. G. Taylor, M. B. Hursthouse and M. E. Light, *Angew. Chem., Int. Ed.*, 2003, **42**, 3488.
15 T. Lin, C. He and Y. Xiao, *J. Phys. Chem. B*, 2003, **107**, 13788.
16 D. A. Wann, R. J. Less, F. Rataboul, P. D. McCaffrey, A. M. Reilly, H. E. Robertson, P. D. Lickiss and D. W. H. Rankin, *Organometallics*, 2008, **27**, 4183.
17 F. J. Feher and T. A. Budzichowski, *J. Organomet. Chem.*, 1989, **373**, 153.
18 C. Pakjamsai and Y. Kawakami, *Des. Monomers Polym.*, 2005, **8**, 423.
19 F. J. Feher and T. A. Budzichowski, *J. Organomet. Chem.*, 1989, **379**, 33.
20 A. D. Becke, *J. Chem. Phys.*, 1993, **98**, 5648; C. Lee, W. Yang and R. G. Parr, *Phys. Rev. B: Condens. Matter*, 1988, **37**, 785.
21 R. Ditchfield, W. J. Hehre and J. A. Pople, *J. Chem. Phys.*, 1971, **54**, 724; W. J. Hehre, R. Ditchfield and J. A. Pople, *J. Chem. Phys.*, 1972, **56**, 2257; M. M. Francl, W. J. Pietro, W. J. Hehre, J. S. Binkley, M. S. Gordon, D. J. DeFrees and J. A. Pople, *J. Chem. Phys.*, 1982, **77**, 3654.
22 T. H. Dunning, Jr., *J. Chem. Phys.*, 1989, **90**, 1007; D. E. Woon and T. H. Dunning, Jr., *J. Chem. Phys.*, 1993, **98**, 1358.
23 D. Feller, *J. Comp. Chem.*, 1996, **17**, 1571; K. L. Schuchardt, B. T. Didier, T. Elsethagen, L. Sun, V. Gurumoorthi, J. Chase, J. Li and T. L. Windus, *J. Chem. Inf. Model.*, 2007, **47**, 1045.
24 A. A. Granovsky, *PC GAMESS version 7.0*, http://classic.chem.msu.su/gran/gamess/index.html.
25 M. W. Schmidt, K. K. Baldridge, J. A. Boatz, S. T. Elbert, M. S. Gordon, J. J. Jensen, S. Koseki, N. Matsunaga, K. A. Nguyen, S. Su, T. L. Windus, M. Dupuis and J. A. Montgomery, *J. Comput. Chem.*, 1993, **14**, 1347.
26 G. V. Girichev, A. N. Utkin and Yu. F. Revichev, *Prib. Tekh. Eksp.*, 1984, **2**, 187; G. V. Girichev, S. A. Shlykov and Yu. F. Revichev, *Prib. Tekh. Eksp.*, 1986, **4**, 167; S. A. Shlykov and G. V. Girichev, *Prib. Tekh. Eksp.*, 1988, **6**, 141.
27 H. Fleischer, D. A. Wann, S. L. Hinchley, K. B. Borisenko, J. R. Lewis, R. J. Mawhorter, H. E. Robertson and D. W. H. Rankin, *Dalton Trans.*, 2005, 3221.
28 A. V. Zakharov and Yu. A. Zhabanov, *J. Mol. Struct.*, 2010, DOI: 10.1016/j.molstruc.2010.01.013.
29 B. Anderson, H. M. Seip, T. G. Strand and R. Stølevik, *Acta Chem. Scand.*, 1969, **23**, 3224.
30 A. W. Ross, M. Fink and R. Hilderbrandt, *International Tables for Crystallography, Vol. C*, Kluwer Academic Publishers, Dordrecht, The Netherlands, 1992.
31 I. Hargittai, *A Survey: The Gas-Phase Electron Diffraction Technique of Molecular Structure Determination in Stereochemical Applications of Gas-Phase Electron Diffraction, Part A* (ed. I. Hargittai and M. Hargittai), VCH Publishers, Weinheim, Germany, 1988.
32 P. D. McCaffrey, J. K. Dewhurst, D. W. H. Rankin, R. J. Mawhorter and S. Sharma, *J. Chem. Phys.*, 2008, **128**, 204304.
33 D. A. Wann, A. V. Zakharov, A. M. Reilly, P. D. McCaffrey and D. W. H. Rankin, *J. Phys. Chem. A*, 2009, **113**, 9511.
34 D. A. Wann, F. Rataboul, A. M. Reilly, H. E. Robertson, P. D. Lickiss and D. W. H. Rankin, *Dalton Trans.*, 2009, 6843.
35 D. A. Wann, A. M. Reilly, F. Rataboul, P. D. Lickiss and D. W. H. Rankin, *Z. Naturforsch. B*, 2009, **64**, 1269.
36 EaStCHEM Research Computing Facility (http://www.eastchem.ac.uk/rcf). This facility is partially supported by the eDIKT initiative (http://www.edikt.org).
37 J. VandeVondele, M. Krack, F. Mohamed, M. Parrinello, T. Chassaing and J. Hutter, *Comput. Phys. Commun.*, 2005, **167**, 103.
38 J. J. P. Stewart, *J. Mol. Model.*, 2007, **13**, 1173.
39 G. Bussi, D. Donadio and M. Parrinello, *J. Chem. Phys.*, 2007, **126**, 014101.
40 K. Larsson, *Ark. Kemi*, 1960, **16**, 209.
41 J. C. Clark, S. Saengkerdsub, G. T. Eldridge, C. Campana and C. E. Barnes, *J. Organomet. Chem.*, 2006, **691**, 3213.
42 A. R. Bassindale, D. J. Parker, M. Pourny, P. G. Taylor, P. N. Horton and M. B. Hursthouse, *Organometallics*, 2004, **23**, 4400.
43 Y. Kawakami, K. Yamaguchi, T. Yokozawa, T. Serizawa, M. Hasegawa and Y. Kabe, *Chem. Lett.*, 2007, **36**, 792.
44 R. Tacke, A. Lopez-Mras, W. S. Sheldrick and A. Sebald, *Z. Anorg. Allg. Chem.*, 1993, **619**, 347.
45 A. L. Spek, (2008) *PLATON, A Multipurpose Crystallographic Tool*, Utrecht University, Utrecht, The Netherlands; See also A. L. Spek, *J. Appl. Cryst.*, 2003, 36, 7.

